
Princeton Plasma Physics Laboratory

PPPL-

PPPL-



Prepared for the U.S. Department of Energy under Contract DE-AC02-09CH11466.

Princeton Plasma Physics Laboratory

Report Disclaimers

Full Legal Disclaimer

This report was prepared as an account of work sponsored by an agency of the United States Government. Neither the United States Government nor any agency thereof, nor any of their employees, nor any of their contractors, subcontractors or their employees, makes any warranty, express or implied, or assumes any legal liability or responsibility for the accuracy, completeness, or any third party's use or the results of such use of any information, apparatus, product, or process disclosed, or represents that its use would not infringe privately owned rights. Reference herein to any specific commercial product, process, or service by trade name, trademark, manufacturer, or otherwise, does not necessarily constitute or imply its endorsement, recommendation, or favoring by the United States Government or any agency thereof or its contractors or subcontractors. The views and opinions of authors expressed herein do not necessarily state or reflect those of the United States Government or any agency thereof.

Trademark Disclaimer

Reference herein to any specific commercial product, process, or service by trade name, trademark, manufacturer, or otherwise, does not necessarily constitute or imply its endorsement, recommendation, or favoring by the United States Government or any agency thereof or its contractors or subcontractors.

PPPL Report Availability

Princeton Plasma Physics Laboratory:

<http://www.pppl.gov/techreports.cfm>

Office of Scientific and Technical Information (OSTI):

<http://www.osti.gov/bridge>

Related Links:

[U.S. Department of Energy](#)

[Office of Scientific and Technical Information](#)

[Fusion Links](#)

Pedestal fueling simulations with a coupled kinetic-kinetic plasma-neutral transport code

D. P. Stotler^{a,*}, C. S. Chang^a, S. H. Ku^a, J. Lang^a,
G. Y. Park^b

^a*Princeton Plasma Physics Laboratory, Princeton University, P. O. Box 451,
Princeton, NJ 08543-0451, USA*

^b*National Fusion Research Institute, Daejeon, Korea*

Abstract

A Monte Carlo neutral transport routine, based on DEGAS2, has been coupled to the guiding center ion-electron-neutral neoclassical PIC code XGC0 to provide a realistic treatment of neutral atoms and molecules in the tokamak edge plasma. The DEGAS2 routine allows detailed atomic physics and plasma-material interaction processes to be incorporated into these simulations. The spatial profile of the neutral particle source used in the DEGAS2 routine is determined from the fluxes of XGC0 ions to the material surfaces. The kinetic-kinetic plasma-neutral transport capability is demonstrated with example pedestal fueling simulations.

Key words: (PSI-20) DEGAS, Neutrals, Edge Modeling, Edge Pedestal, Recycling
PACS: 52.25.Ya, 52.55.Fa, 52.65.Pp, 52.65.Rr

1 Introduction

ITER's performance is expected to be sensitive to the plasma parameters at the top of the pedestal. To increase our confidence in predicting those pedestal parameters, extensive experimental and theoretical research efforts have been undertaken

* Corresponding and presenting author
Email address: dstotler@pppl.gov (D. P. Stotler).

to understand the physical processes governing the buildup and structure of the pedestal in the inter-ELM phase of the H-mode.

One need is to determine the role of neoclassical processes in the pedestal, rendered significant by the reduced anomalous transport in H-mode. However, the characteristics of the H-mode pedestal complicate the development of analytic neoclassical models: plasma gradient scale lengths are comparable to the ion banana orbit width, the magnetic separatrix is nearby, and single particle loss holes exist in ion velocity space.

These complications led Chang et al. [1] to develop the kinetic, guiding center ion, neoclassical, PIC code XGC0. In [1], they examined the effects of self-consistent radial electric fields and collisions on pedestal characteristics and also demonstrated pedestal buildup due to ionization of recycled neutrals via a simplified neutral routine built into XGC0. Subsequently, XGC0 has been extended to include kinetic electrons, impurity ions, a logical sheath, and three-dimensional magnetic perturbations [2]. Among recent applications are the simulation of the ELM cycle by coupling to the nonlinear MHD code, M3D [3] and determination of the neoclassical scaling of the divertor heat load width [4]. Planned code upgrades will treat multiple charge state impurity species and two-dimensional variation for the electrostatic potential.

Previously, the behavior of neutrals in H-mode has been examined via comprehensive Monte Carlo neutral transport codes coupled to two-dimensional fluid edge plasma codes, e.g., [5,6]. However, the applicability of the fluid approximation to the pedestal, scrape-off layer, and divertor plasma has been called into question [7]. The XGC0 code in contrast provides a kinetic treatment of ions and electrons and naturally incorporates a kinetically self-consistent radial electric field and rotation. To render the treatment of neutrals in XGC0 comparable to that used with the fluid plasma codes, we have replaced its built-in, simplified neutral transport routine with one based on the DEGAS2 Monte Carlo neutral transport code [8]. The resulting coupled code resolves neutral quantities throughout the entire vacuum vessel and allows neutral sources to be placed at material surfaces, where they can be determined via realistic plasma-material interaction models. Plasma-neutral collisions interactions are characterized using DEGAS2's atomic physics machinery and database. Synthetic diagnostics based on neutral phenomena, e.g., visible cameras, can be applied to any simulation via the existing DEGAS2 routine. Although XGC0's simplified, built-in neutral transport routine includes the interactions of kinetic electrons and impurities with the neutral background, we have not enabled those capabilities for the XGC0-DEGAS2 simulations described here since their verification is still underway.

2 Approach to Kinetic-Kinetic Plasma-Neutral Coupling

The most widely used coupled tokamak edge and scrape-off layer fluid plasma - Monte Carlo neutral code is B2-EIRENE [9,10], although others exist, e.g., UEDGE-DEGAS2 [11]. The neutral code computes sources of plasma mass, momentum, and energy due to neutral-plasma interactions. Those sources are returned to the fluid plasma code and used as the right-hand sides of its plasma transport equations. Because kinetic information is lost with this approach, adapting it to a kinetic plasma code such as XGC0 is problematic. The most comprehensive alternative, equivalent to Direct Simulation Monte Carlo [12], would be to have a single code track both charged and neutral particles. However, obtaining adequate atomic interaction statistics over the entire tokamak plasma with such a code would require many more computational resources than with the present method.

We instead use an approach related to the “test particle Monte Carlo” method [13] in which individual test particles collide with a background characterized by a specified distribution function. In the nonlinear case, the distribution is updated in iterative fashion to convergence. The accuracy of this method hinges on the adequacy of the chosen representation for the background distribution function.

Implementation of this approach in XGC0-DEGAS2 requires two complementary plasma-neutral atomic collision operators, one embedded in XGC0 and one in DEGAS2. For the rest of this paper, we will refer to the implementation of these atomic collision operators as the “XGC0” and “DEGAS2” atomic collision routines; Each replaces a corresponding routine in XGC0’s simplified, built-in neutral transport routine.

This initial version of XGC0-DEGAS2 uses a drifting Maxwellian for the background distributions and the routines exchange the fluid moments (density, three-dimensional flow velocity, and temperature) obtained by integrating the local distribution function over each cell in the computational mesh. Additional details of this algorithm and its conservation properties will be described elsewhere.

The computational mesh for the plasma-neutral coupling is based on a 2-D, quasi-orthogonal grid with one coordinate aligned with flux surfaces so as to allow sharp radial gradients to be efficiently resolved [14]. The required poloidal flux values are obtained from a particular EFIT equilibrium calculation [15]. Since the outer boundary of this mesh does not coincide everywhere with the vacuum vessel boundary, we tile the intervening volume with triangles [16]; the size of these triangles is

controlled in part by a user specified discretization of the boundary. The quadrilaterals of the flux surface following mesh are then sub-divided into two triangles so that the entire geometry consists of an unstructured, triangular mesh. To facilitate conservation of mass, momentum, and energy, all quantities resolved on this mesh, in both codes, are integrated over the volume of these triangles.

The implementation of plasma-neutral collisions in the DEGAS2 routine is as in previous DEGAS2 applications [8]. In the XGC0 routine, a modified null collision technique [17] is used to process collisions of the kinetic XGC0 ions with the fluid neutral background provided by DEGAS2. For the example simulations described here, ionization is processed using the ion locations and a fixed electron temperature profile; the kinetic electron capability will be demonstrated in future simulations. The ionization rate [18,19] and velocity dependent charge exchange cross section [20] are obtained via DEGAS2's atomic physics routines and tables. Note that planned physics improvements to XGC0-DEGAS2, e.g., addition of impurities and molecules, primarily involve extensions of the XGC0 routine since the DEGAS2 routine already has the requisite capabilities.

The primary neutral source for the DEGAS2 routine is provided by the recycling of XGC0 ions crossing the vacuum vessel boundary. The poloidal distribution of those ions is compiled by XGC0 and used periodically to update the neutral source profile transferred to DEGAS2. The integrated source current is set equal to the total current of ions that have crossed the vessel boundary since the previous call to the DEGAS2 routine. A future version of this algorithm will similarly compile the energy distribution of the boundary crossing ions and transfer it to DEGAS2. The DEGAS2 routine can then sample the incident energy of recycling ions from that distribution, allowing detailed plasma-material interaction models to be employed in determining the kinetic characteristics of the neutral source. For the present work, the source simply consists of 3 eV D atoms with a cosine angular distribution relative to the surface normal, as if surface generated molecules were dissociated near the surface.

Since the neutral transport and evolution times are not short compared with the time between calls to the DEGAS2 routine (typically 15 μ s), the periodic neutral transport calculations are performed in a time dependent manner [21] and the resulting moments of the neutral distribution function are integrated over the time interval. In addition to sampling from the recycling neutral source, the DEGAS2 routine also samples from the neutral distribution within the volume at the end of the previous call.

XGC0 scales very efficiently on massively parallel computers, up to peta-flop lev-

els. However, the simulations described in the next section are performed on a smaller, local Linux cluster utilizing 32 cores on 8 nodes, a practical amount of computational power given that we are not using the code’s kinetic electron capability. About 17 hours are required to process the 10,000 time steps in these runs. A total of 7.6 million ions and 0.96 million neutral particles are tracked through the 17,325 mesh cells in the geometry used for the plasma-neutral calculation. Less than 1 GB of memory is needed on each core.

3 Demonstration of the Coupled XGC0-DEGAS2 Code

These simulations are based on DIII-D discharge 96333 [5]. The EFIT equilibrium for this shot at 3300 milliseconds has served as a standard reference discharge for XGC simulations[22,23]. As in those papers, we assume initial H-mode like profiles with a pedestal density of $5 \times 10^{19} \text{ m}^{-3}$ and a temperature of 1 keV. However, for the present simulations we employ a somewhat lower electron temperature, Fig. 1(b), consistent with DIII-D H-mode profiles at this density (e.g., [24]). The only other adjustable parameters in these simulations are the 90% recycling coefficient, enforced by the DEGAS2 routine, and a collisionless gyroviscosity coefficient of $5 \times 10^{-2} \text{ m}^2/\text{s}$ used by XGC0 in pushing its ions.

The ion marker particles are tracked for 20 ion transit times (1.56 ms) until all transients have died off. The density pedestal builds up and the gradients steepens, as in [1]. Note that the ion temperature drops from its initial value of 1 keV at the top of the pedestal since we have, for simplicity, not included a heat source from the core to offset the ion heat loss to the boundary and neutral cooling. More detailed XGC0-DEGAS2 simulations of particular experimental discharges would include an appropriate heat source, kinetic electrons, impurity species, logical sheath, as well as turbulent diffusion with an experimentally calibrated anomalous diffusion coefficient.

The ion fluxes to the divertor floor are plotted in Fig. 2 as a function of distance along the boundary. These ion losses are solely due to ion motion along and across the open field lines as well as to ion orbits intersecting the material boundary, with the latter occurring primarily in the low poloidal field region around the X-point [1]. In the baseline simulation, this ion flux profile is passed to DEGAS2 and used to specify the poloidal distribution of the neutral recycling source (the “divertor peaked” source). As a contrasting example, we perform a second simulation in which the neutral source is instead spread uniformly over the entire boundary. The results of this run are relevant to other fueling scenarios, e.g., due to main chamber

recycling or gas puffing and is reminiscent of the “puff and pump” approach [25].

Almost all neutrals in the divertor peaked run are ionized in the divertor, Fig. 3(a); the ionization rate integrated over the core plasma is only 9% of the neutral source current. In the poloidally uniform recycling case, Fig. 3(b), this fraction increases to 47% since the neutrals have to travel, on average, a shorter distance to reach the separatrix than they do in coming from the divertor. Even though the physics in these simulations is limited, the integrated divertor ion currents [$3.1 \times 10^{22} \text{ s}^{-1}$ (divertor peaked), $1.5 \times 10^{22} \text{ s}^{-1}$ (uniform)] and core ion source rates [$2.4 \times 10^{21} \text{ s}^{-1}$ (divertor peaked), $5.4 \times 10^{21} \text{ s}^{-1}$ (uniform)] are comparable to the analogous values inferred by Owen [5] in more detailed modeling of similar discharges.

The divertor peaked source results in a 25% increase in the ion density at the pedestal top [Fig. 1(a) at $\psi/\psi_{\text{sep}} = 0.99$] relative to the initial profile. As one would expect, the uniform source yields a larger increase, 41%. The ion temperature profiles also differ since the core charge exchange losses are considerably larger in the poloidally uniform recycling simulation 0.3 MW vs. 0.08 MW with divertor peaked recycling. These are 47% and 16%, respectively, of the losses integrated over the entire volume. The core losses associated with ionization are much smaller, 21 kW with uniform recycling and 9 kW for divertor peaked recycling.

The change in recycling also affects the flux surface averaged toroidal and poloidal flow velocities, Fig. 4. Earlier XGC0 simulations with L-mode profiles (using the simplified neutral transport model) [26] obtained a more dramatic result. Namely, that placing the neutral source on the high field side of the device led to greater toroidal rotation speeds, consistent with easier access to H-mode, than found with it on the low field side.

As a sensitivity test, we perform a second pair of simulations with an electron temperature profile equal to the initial ion temperature profile, i.e., a pedestal temperature of 1 keV and SOL value of 100 eV. This mainly leads to increased ionization in the divertor (for divertor peaked recycling) or scrape-off layer (uniform source). The other results are qualitatively similar to those quoted above.

4 Concluding Remarks

We have described the kinetic-kinetic plasma-neutral code obtained by coupling the guiding center, ion-electron-neoclassical PIC code XGC0. Example DIII-D H-mode particle fueling simulations showed that a poloidally uniform neutral source

provided much more core fueling than one peaked in the divertor. These XGC0-DEGAS2 simulations are improved versions of those documented by Wan [23] and yield similar neutral to ion temperature ratios. Future simulations with additional physics will be used in more detailed validation exercises against particular experimental discharges.

In parallel with this work, the impact of neutrals on ion temperature gradient and trapped electron mode driven turbulence are being investigated via the simplified 2-D Monte Carlo neutral transport model incorporated into the XGC1 gyrokinetic turbulence code [27]. The ion cooling due to neutral charge exchange widens the ion temperature pedestal width through radial orbit spreading and produces ITG turbulence at the density pedestal top. Thus, an increased neutral density reduces the $\vec{E} \times \vec{B}$ shearing rate to allow stronger turbulence in the pedestal. This result is consistent with the higher L-H transition power required with higher levels of neutral recycling. As was done with XGC0, we plan to replace this neutral routine with the one based on DEGAS2.

Acknowledgments

This work is supported by U.S. DOE Contract DE-AC02-09CH11466.

References

- [1] C. S. Chang, S. Ku, H. Weitzner, *Phys. Plasmas* 11 (2004) 2649.
- [2] G. Park et al., *Phys. Plasmas* 17 (2010) 102503.
- [3] G. Park et al., *J. Physics: Conf. Series* 78 (2007) 012087.
- [4] A. Y. Pankin et al., presented at the 23rd IAEA Fusion Energy Conference, Daejeon, Korea, October 11 – 16, 2010 (2010).
- [5] L. W. Owen et al., *J. Nucl. Mater.* 290–293 (2001) 464.
- [6] A. Loarte et al., *J. Nucl. Mater.* 266–269 (1999) 1123.
- [7] M. Wischmeier et al., *J. Nucl. Mater.* 415 (2011) S523.
- [8] D. P. Stotler, C. F. F. Karney, *Contrib. Plasma Phys.* 34 (1994) 392.
- [9] D. Reiter, *J. Nucl. Mater.* 196–198 (1992) 80.

- [10] R. Schneider et al., *Contrib. Plasma Phys.* 46 (2006) 3.
- [11] D. P. Stotler et al., *Contrib. Plasma Phys.* 40 (2000) 221.
- [12] *Molecular Gas Dynamics*, Clarendon Press, Oxford, 1976.
- [13] J. K. Haviland, M. L. Lavin, *Phys. Fluids* 5 (1962) 1399.
- [14] R. Marchand, M. Dumbery, *Comput. Phys. Comm.* 96 (1996) 232.
- [15] L. L. Lao et al., *Nucl. Fusion* 25 (1985) 1611.
- [16] J. R. Shewchuck, in: *Applied Computational Geometry: Towards Geometric Engineering*, Vol. 1148, Springer, New York, 1996, p. 203.
- [17] H. R. Skullerud, *J. Phys. D: Appl. Phys.* 1 (1968) 1567.
- [18] S. D. Loch et al., *Plasma Phys. Control. Fusion* 51 (2009) 105006.
- [19] DEGAS2 User's Manual, http://w3.pppl.gov/degas2/Doc/degas2_all.pdf.
- [20] P. S. Krstic, D. R. Schultz, *At. Plasma-Mater. Data Fus.* 8 (1998) 1.
- [21] D. Reiter et al., *J. Nucl. Mater.* 220–222 (1995) 987.
- [22] X. Q. Xu et al., *Nucl. Fusion* 49 (2009) 065023.
- [23] W. Wan et al., *Phys. Plasmas* 18 (2011) 056116.
- [24] A. W. Leonard et al., *J. Nucl. Mater.* 363–365 (2007) 1066.
- [25] M. A. Mahdavi et al., *Nucl. Fusion* 42 (2002) 52.
- [26] R. Maingi et al., *Plasma Phys. Control. Fusion* 46 (2004) A305.
- [27] C. S. Chang et al., *Phys. Plasmas* 16 (2009) 056108.

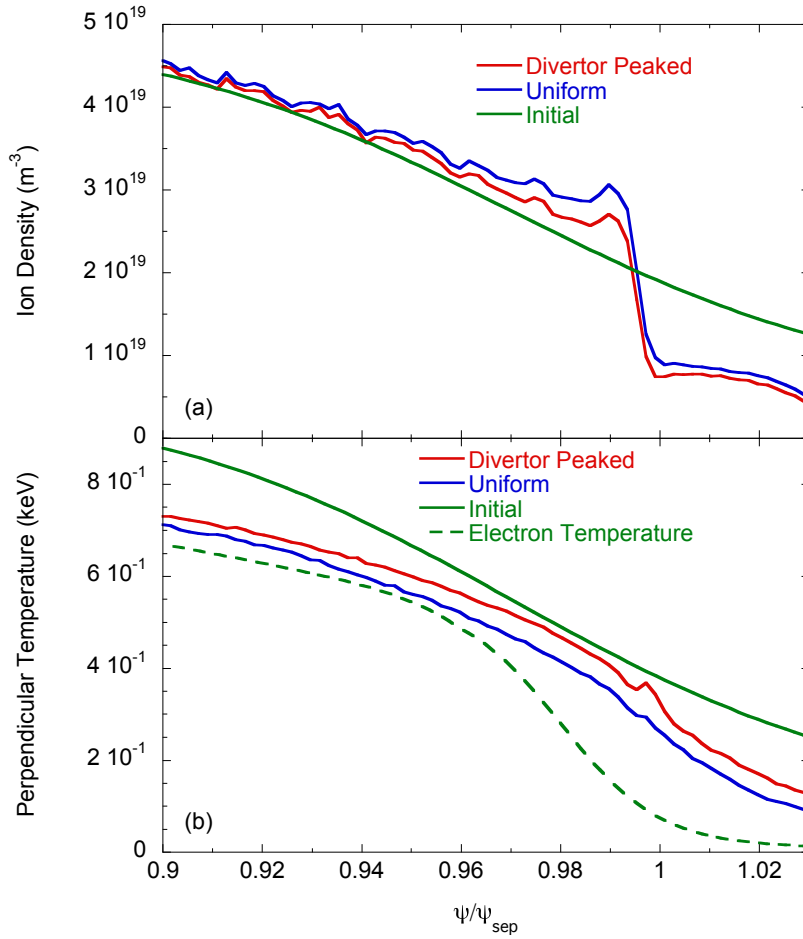


Figure 1. Ion density (a) and temperature profiles (b) in runs with divertor peaked and uniform recycling. The fixed electron temperature for both runs is also plotted.

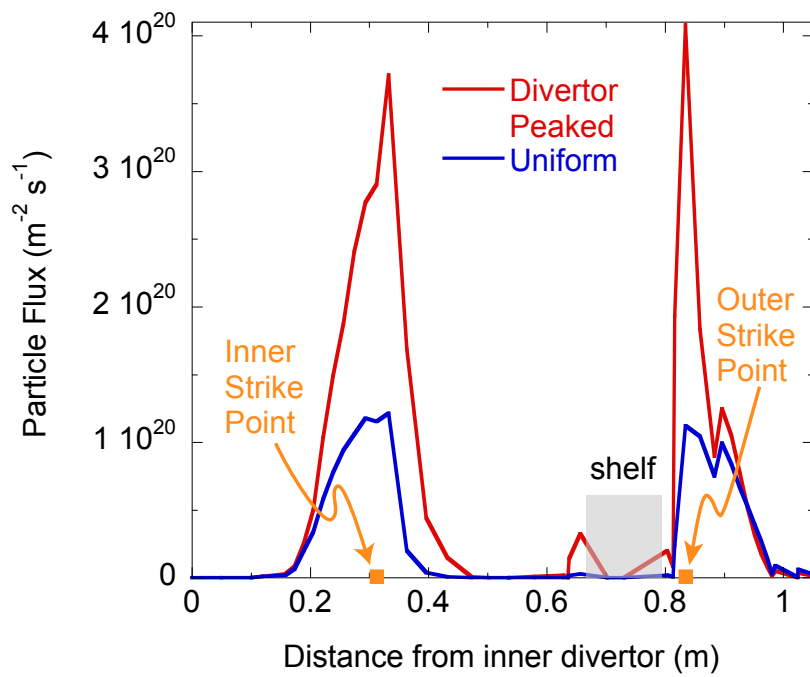


Figure 2. Particle flux to divertor as a function of distance along the boundary from the the inner divertor for the divertor peaked and uniform recycling runs. The shaded region corresponds to the “shelf” region of DIII-D’s outer divertor that is shielded from the core plasma.

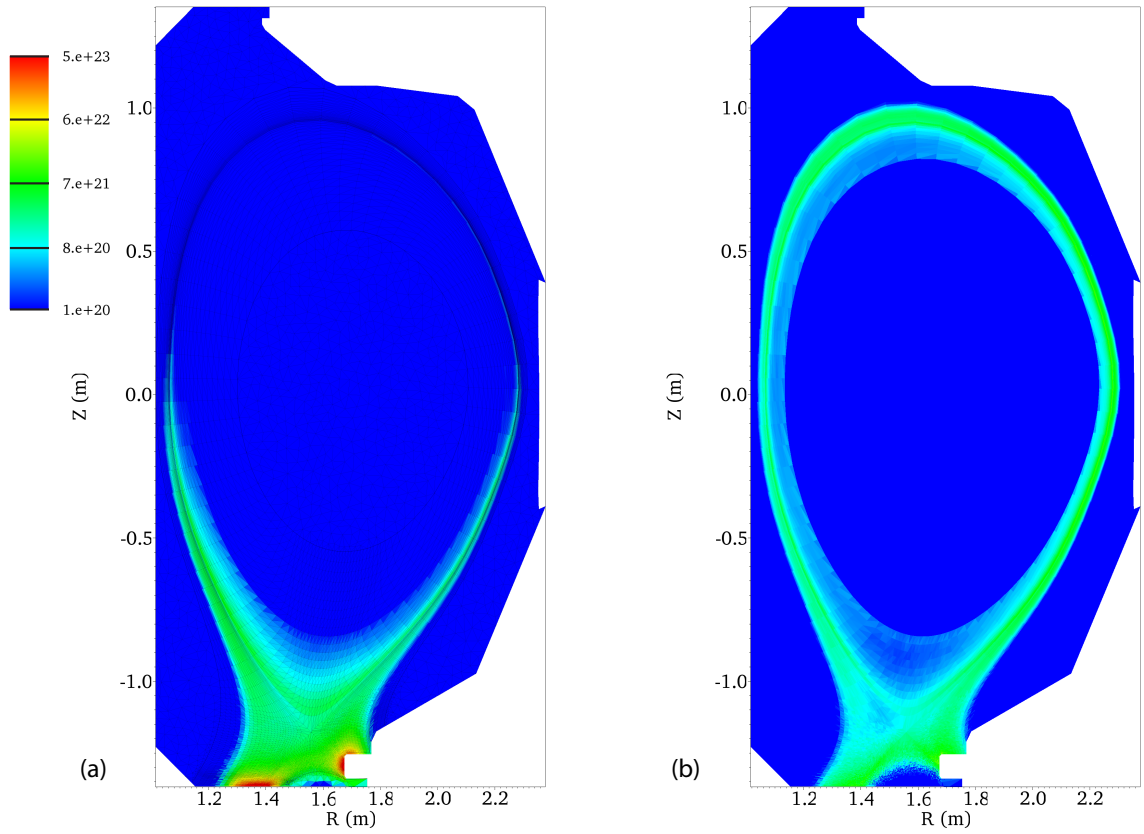


Figure 3. Ion source due to neutrals in (a) divertor peaked and (b) poloidally uniform recycling simulations. The computational mesh used for the plasma-neutral coupling is overlaid in (a).

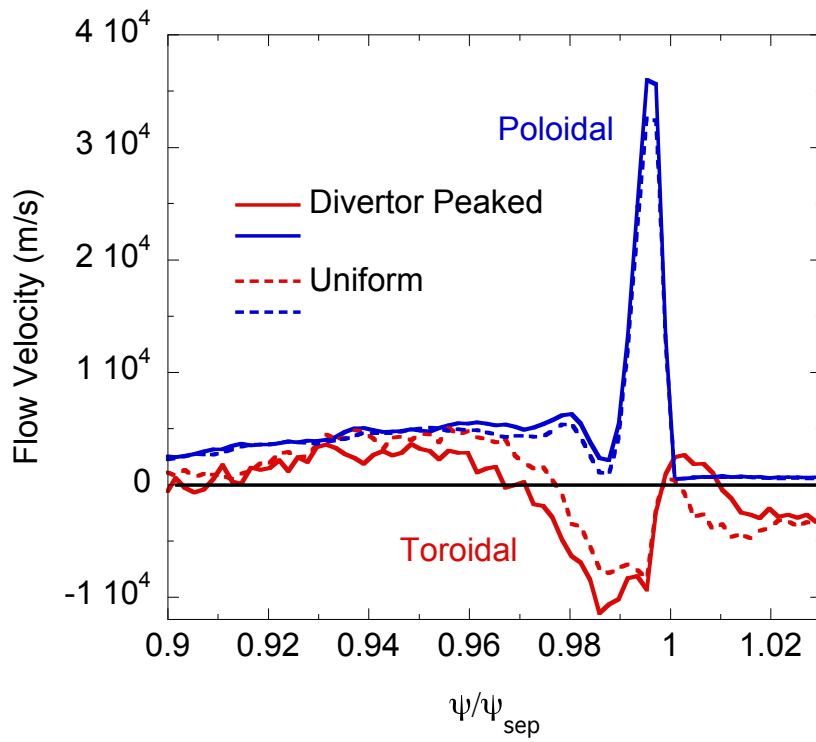


Figure 4. Ion toroidal flow velocity and $\vec{E} \times \vec{B}$ poloidal velocity for the divertor peaked and uniform recycling runs.

The Princeton Plasma Physics Laboratory is operated
by Princeton University under contract
with the U.S. Department of Energy.

Information Services
Princeton Plasma Physics Laboratory
P.O. Box 451
Princeton, NJ 08543

Phone: 609-243-2245
Fax: 609-243-2751
e-mail: pppl_info@pppl.gov
Internet Address: <http://www.pppl.gov>